

Unified quantitative model for magnetic and electronic spectra of the undoped cuprates

B. Dalla Piazza,¹ M. Mourigal,^{1,2} M. Guarise,³ H. Berger,³ T. Schmitt,⁴ M. Grioni,³ and H. M. Rønnow¹

¹Laboratory for Quantum Magnetism, École Polytechnique Fédérale de Lausanne (EPFL), CH-1015, Switzerland

²Institut Laue-Langevin, BP 156, 38042 Grenoble Cedex 9, France

³Laboratory of Photoelectron Spectroscopy, École Polytechnique Fédérale de Lausanne (EPFL), CH-1015, Switzerland

⁴Swiss Light Source, Paul Scherrer Institut, CH-5232 Villigen PSI, Switzerland

(Dated: November 24, 2021)

Using low-energy projection of the one-band t - t' - t'' -Hubbard model we derive an effective spin-Hamiltonian and its spin-wave expansion to order $1/S$. We fit the spin-wave dispersion of several parent compounds to the high-temperature superconducting cuprates: La_2CuO_4 , $\text{Sr}_2\text{CuO}_2\text{Cl}_2$ and $\text{Bi}_2\text{Sr}_2\text{YCu}_2\text{O}_8$. Our accurate quantitative determination of the one-band Hubbard model parameters allows prediction and comparison to experimental results of measurable quantities such as staggered moment, double occupancy density, spin-wave velocity and bimagnon excitation spectrum and density of states, which is discussed in relation to K-edge RIXS and Raman experiments.

PACS numbers: 74.72.Cj, 75.30.Ds, 78.70.Ck

High- T_c superconductors challenge all known theoretical approaches by mixing charge and magnetic degrees of freedom and lacking a small variational parameter. The One-Band Hubbard Model (1bHub), proposed by Anderson [1] to describe their CuO_2 planes, includes both of these difficulties in its parameters, the electron filling, the hopping matrix element t and the Coulomb repulsion U . The ratio t/U is moderately small in the cuprates, thus most approaches start by projecting out double occupancies (DO) to obtain the Heisenberg model at half-filling or the t - J model for hole- or electron-doping. Such a projection is too complicated to be carried out exactly but may be performed as an expansion in powers of t/U [2].

Experimentally, different techniques have probed separate channels – magnetic or electronic. Inelastic Neutron Scattering (INS) on La_2CuO_4 [3] demonstrated that the projection must be carried out at least to the fourth order (t^4/U^3) to reproduce the observed magnetic excitation spectrum. Angle-Resolved Photo-Emission Spectroscopy (ARPES) indicates that first, second and third nearest neighbor hopping matrix elements are needed to reproduce the observed electronic quasiparticle dispersion [4]. A quantitative description of the undoped high- T_c parent compounds therefore needs a model incorporating both those considerations [5].

In this letter, we develop such a quantitative theory and present the resulting sets of 1bHub parameters for single and bilayer undoped cuprates $\text{Sr}_2\text{CuO}_2\text{Cl}_2$ [6], La_2CuO_4 [7] and $\text{Bi}_2\text{Sr}_2\text{YCu}_2\text{O}_8$ [this work], obtained by fitting their magnetic excitation spectra measured by Resonant Inelastic X-ray Scattering (RIXS) and INS.

We start from the 1bHub Hamiltonian given by

$$\hat{H} = - \sum_{i,j,\sigma} t_{ij} c_{i,\sigma}^\dagger c_{j,\sigma} + U \sum_i n_{i,\uparrow} n_{i,\downarrow} \quad (1)$$

where $c_{i,\sigma}^\dagger$ and $c_{i,\sigma}$ creates or destroys a fermion with spin σ on site i , t_{ij} is the hopping matrix element between

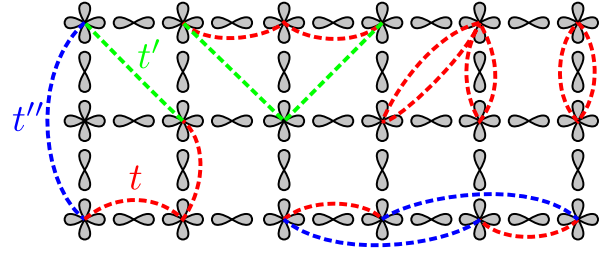


FIG. 1. (Color Online) CuO_2 planes from the perovskite structure. Examples of exchange loops from the effective spin Hamiltonian of Eq. 2 are indicated with first, second and third nearest neighbor hoppings t , t' and t'' .

sites i and j , U the effective on-site repulsion and $n_{i,\sigma} = c_{i,\sigma}^\dagger c_{i,\sigma}$ the fermionic number operator. At half filling, the kinetic term mixes states with different number of DO, which in the limit $t/U \ll 1$ separate into different energy scales. We use the unitary transformation technique [2] up to order t^4/U^3 to decouple these states and obtain the effective spin Hamiltonian

$$\begin{aligned} \hat{H}^{(4)} = & \sum_{\{\overline{12}\}} \left(\frac{4t_{12}^2}{U} - \frac{16t_{12}^4}{U^3} \right) \mathbf{S}_1 \mathbf{S}_2 + \sum_{\{\overline{123}\}} \frac{4t_{12}^2 t_{23}^2}{U^3} \mathbf{S}_1 \mathbf{S}_3 \\ & - \sum_{\{\overline{1234}\}} \frac{4t_{12} t_{23} t_{34} t_{41}}{U^3} \left\{ \sum_{\substack{i,j=1 \\ i \neq j}}^4 \mathbf{S}_i \mathbf{S}_j - 20 \left[(\mathbf{S}_1 \mathbf{S}_2) (\mathbf{S}_3 \mathbf{S}_4) \right. \right. \\ & \left. \left. + (\mathbf{S}_1 \mathbf{S}_4) (\mathbf{S}_2 \mathbf{S}_3) - (\mathbf{S}_1 \mathbf{S}_3) (\mathbf{S}_2 \mathbf{S}_4) \right] \right\} + E^{(4)}, \quad (2) \end{aligned}$$

where $E^{(4)}$ is a constant and $\{\overline{12}\}$, $\{\overline{123}\}$ and $\{\overline{1234}\}$ stand for the plaquette ensembles of two, three and four sites respectively, and connected as sketched. We emphasize that the loop ensembles are fully defined by the considered hopping matrix elements t_{ij} and the lattice topology, so that the Hamiltonian of Eq. 2 is the gen-

eral low-energy projection to order t^4/U^3 of the 1bHub at half filling for any lattice. Examples of plaquettes of two, three and four sites involving first, second and third Nearest Neighbor (NN) hopping amplitudes t , t' and t'' are sketched on Fig. 1. A similar development but away from half-filling would result in a t - J model with the same magnetic couplings as in Eq. 2 plus a family of charge plaquette hoppings. Being the canonical model for high- T_c superconductors, a large variety of analytic and numerical approaches exist to study such a model [8].

In contrast to the doped compounds, the derivation of measurable quantities is much easier for their undoped parents. Here, we use Spin-Wave Theory (SWT) to derive the dispersion of the magnetic excitations which are measured by INS or RIXS. We expand the spin operators of Eq. 2 in terms of Holstein-Primakov bosons. Keeping the first $1/S$ correction for the t_{ij}^2/U terms, the Hamiltonian transforms as $\hat{\mathcal{H}}^{(4)} = E_N + \hat{\mathcal{H}}_2 + \hat{\mathcal{H}}_4 + \mathcal{O}(1/S)$, where the Néel ground-state energy E_N includes the constant of Eq. 2, and the harmonic dispersion $\omega_0(\mathbf{k})$ is obtained from a Bogoliubov transformation of the quadratic term $\hat{\mathcal{H}}_2$. A Hartree-Fock decoupling [9] of the quartic term $\hat{\mathcal{H}}_4$ results in an overall momentum-dependent correction to the magnon energy so that our final spin-wave Hamiltonian reads

$$\hat{\mathcal{H}}^{(4)} = \sum_{\mathbf{k}} Z_c(\mathbf{k}) \omega_0(\mathbf{k}) \alpha_{\mathbf{k}}^\dagger \alpha_{\mathbf{k}} + E_N + \delta E \quad (3)$$

where α 's are free magnon operators, $Z_c(\mathbf{k})$ is the $1/S$ renormalization of their dispersion and δE is the quantum correction to the ground state energy at this order. For the bilayer square-lattice, Eq. 2 is still valid but the loop ensembles now include interlayer hopping t_\perp , and two boson flavors to account for the top and bottom sites. This results in two magnon modes which are gapped respectively at $(0,0)$ and (π,π) but degenerate along the magnetic Zone Boundary (ZB).

Before applying the result to the cuprate compounds SCOC [6] and LCO [7], we report here new measurements of the spin-wave (SW) dispersion in $\text{Bi}_2\text{Sr}_2\text{YCu}_2\text{O}_8$, a bilayer parent compound. Single crystals were grown by the flux method with yttrium ensuring an insulating antiferromagnetic phase. The SW dispersion was measured using Cu L_3 edge RIXS at the SAXES end-station of the Swiss Light Source ADDRESS beamline, experimental details and data analysis as described previously [6].

The spin-wave dispersions of the various compounds are shown in Fig. 2. They all feature a dispersion between the ZB points $(\pi,0)$ and $(\pi/2,\pi/2)$ which can in principle be explained by the effective model of Eq. 2 with NN hopping alone (dashed red lines). However, this approach results in unphysically low $U = 2.2$ eV [3] for LCO and $U < 2$ eV for SCOC and BSYCO. From the former to the latter, their ZB dispersions respectively reach 40, 70 and 55 meV. Although U is an effective on-site repul-

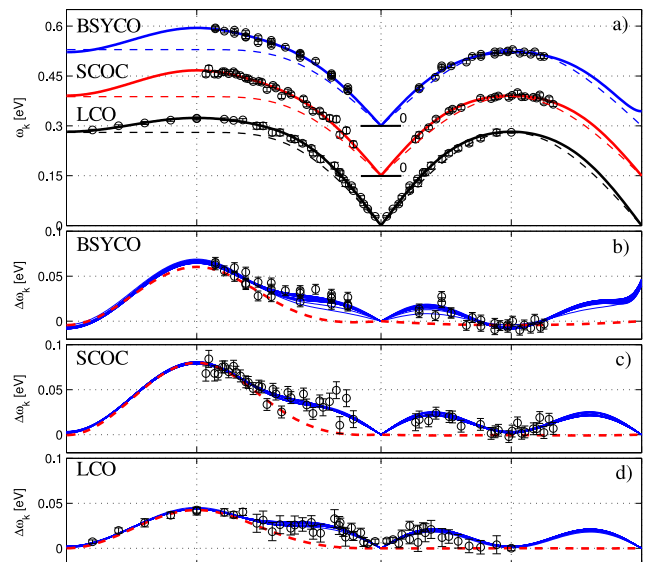


FIG. 2. (Color Online) (a) Fits of the measured SW dispersions (solid lines) and the 1JHei SW dispersion (dashed lines) with $J_{\text{NN}} = \omega_{(\pi/2,\pi/2)}/2Z_c$. From top to bottom: BSYCO ($J_{\text{NN}} = 0.15$ eV), SCOC [6] ($J_{\text{NN}} = 0.12$ eV) and LCO [7] ($J_{\text{NN}} = 0.14$ eV). (b-d) Same as in (a) but subtracted from the 1JHei SW dispersion to enhance details, BSYCO, SCOC and LCO respectively. Data points from experiments are folded onto the equivalent high-symmetry axes of the first Brillouin zone.

sion, closer to the charge-transfer gap than to the bare Coulomb repulsion, a good 1bHub must use an effective parameter compatible with electronic and optical spectroscopies, which request $U \sim 3$ -4 eV for the cuprates [10]. Consistently with ARPES results, we therefore include second and third NN hopping in our effective model and derive the spin-wave dispersion of Eq. 3 which is now a function of four parameters (U, t, t', t''). The measured SW dispersions contain three distinct constraints, the $(\pi,0)$ and $(\pi/2,\pi/2)$ ZB energies and the spin-wave velocity. We thus expect a one-dimensional solution and choose the free parameter to be the effective U . The fitting procedure is as follows. For a fixed choice of $(U, t'/t)$ we start by fitting the two other parameters t/U and t''/t . As the calculation of $1/S$ estimate of Z_c involve a slowly convergent integration over \mathbf{k} -space, we include it in a two-step iterative approach. First, we fix its value to the uniform $Z_0 = 1.1579$ obtained for the NN Heisenberg model (1JHei). Then, we fit $Z_0\omega_{\mathbf{k}}(U, t/U, t'/t, t''/t)$ using a non-linear least-squares algorithm and calculate a first non-uniform $Z_1(\mathbf{k})$ from the obtained parameters set. We iterate this procedure until $Z_n(\mathbf{k})$ converges, typically after 10-15 steps. In the case of BSYCO, we further include an interplane hopping t_\perp . However, the resolution of RIXS does not allow to distinguish the splitting between the two magnon modes and we fix it to the value $t_\perp = 54$ meV reported by Chuang *et al.* [11].

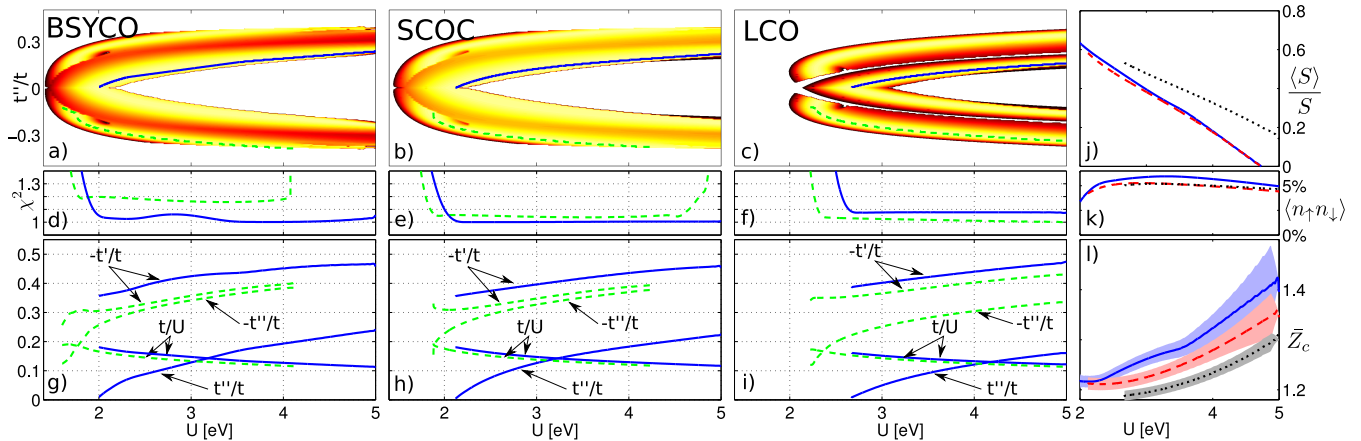


FIG. 3. (Color Online) Summary of the fitting results. (a-c) Goodness (χ^2) of the $(t/U, t'/t)$ fit for fixed $(U, t''/t)$ in the case $\text{Bi}_2\text{Sr}_2\text{CaCu}_2\text{O}_8$, $\text{Sr}_2\text{CuO}_2\text{Cl}_2$ and La_2CuO_4 respectively. Solid (blue) and dashed (green) lines are best fit solutions as function of U for $t''/t < 0$ and $t''/t > 0$ respectively. (d-f) χ^2 along the best fit lines defined in (a-c). (g-i) (U, t, t', t'') solutions along the best fit lines defined in (a-c). (j-l) Staggered magnetization, DO density and \mathbf{k} -averaged quantum $1/S$ renormalization Z_c along the $t''/t < 0$ best fit lines defined in (a-d). Lines: Solid blue BSYCO, dashed red SCOC and dotted black LCO. Shaded areas indicate \mathbf{k} -variation of Z_c .

The fitting results over the $(U, t''/t)$ plane are shown in Fig. 3 with the $(U, t/U, t'/t, t''/t)$ parameters along the best fit lines. Overall, the four compounds share common features *i.e.* a strong lower boundary for U , an increase of $|t'|/t$ and t''/t with U , and a slowly varying t/U . Due to the $t^2 t''/U^3$ term, the calculated magnon dispersion is symmetric in the signs of t and t' but not in the relative sign of t' and t'' resulting in two separate solutions for $t' t'' < 0$ and $t' t'' > 0$. From the best-fit lines, one can see that the inclusion of $|t''|$ is necessary in order to get $U \approx 3$ -4 eV. For some regions of the $(U, t''/t)$ space, the Néel state is not the classical ground state of Eq. 2, and/or it is destroyed by quantum fluctuations. Both cases can be systematically determined by looking at the size of zero-point fluctuations $\langle a_i^\dagger a_i \rangle$. The outermost void regions in Fig. 3(a)-(d) are those where Néel order is unstable. In Fig. 3(m), we calculate the evolution of the staggered magnetization as a function of U along the best fit lines. Increasing U , t' and t'' grow while t/U stays roughly constant, bringing more frustration and subsequently reducing the ordered moment. We calculate the double occupation density using the Feynman-Hellmann theorem $\langle n_{i,\uparrow} n_{i,\downarrow} \rangle = \partial \langle \hat{H}^{(4)} \rangle / \partial U$. Along the best fit lines, a U -independent value 5% is found for all cuprates in agreement with the electronic shielding factor calculated in ref. [12]. The $1/S$ estimate of $Z_c(\mathbf{k})$ is found to vary only about 2% across the Brillouin zone. In Fig. 3(o) we show the average value, which vary from 1.2 to 1.3 for $U \approx 3$ -4 eV which again reveals the prominent role of quantum fluctuations in the range of parameters relevant for the cuprates.

The effective U cannot be directly obtained through magnetic excitations. However, more direct experimen-

	t [meV]	t' [meV]	t'' [meV]	$\langle S \rangle / S$	c [meVÅ]	$\langle n_{i,\uparrow} n_{i,\downarrow} \rangle$
BSYCO	470(10)	-205(3)	79(4)	0.3	0.146	5.9%
SCOC	480(10)	-200(5)	75(5)	0.29	0.163	5.1%
LCO	492(7)	-207(3)	45(2)	0.4	0.195	5.2%

TABLE I. Parameters determined from the spin-wave fits with fixed $U = 3.5$ eV and $t' t'' < 0$.

tal techniques may give good estimates of U thus determining a unique set of 1bHub parameters for each of the above compounds. In particular, an estimate of the 1bHub parameters of SCOC was obtained from ARPES [10] as $U = 3.5$ eV, $t = 0.35$ eV, $t' = -0.12$ eV and $t'' = 0.08$ eV. Consistently with those parameters and in order to compare the three cuprates, we adopt in Tab. I a uniform value $U = 3.5$ eV and the $t' t'' < 0$ solution. A more accurate determination of U could be found in the charge-transfer (CT) excitation part of the RIXS spectrum. Using the above ARPES parameter estimates, Hasan *et al.* could identify a dispersing excitation around 3 eV in Cu K-edge RIXS as CT excitation [13]. A similar approach using our parameter sets would allow unambiguous determination of U .

Having established a quantitative model for the SW dispersion allows to predict further quantities. We compute the non-interacting two-magnon dynamical structure factor $S^{zz}(\mathbf{k}, \omega)$ probed by INS, and the two-magnon density of states (DOS) underlying, at $(0, 0)$, Raman scattering and, at $(\pi, 0)$, K-edge RIXS [14]. Although higher-order magnon interaction affect those two-magnon quantities [15–17] our results already allow several observations. Compared to 1JHei, our predictions show the enhancement of a 500 meV peak in S^{zz}

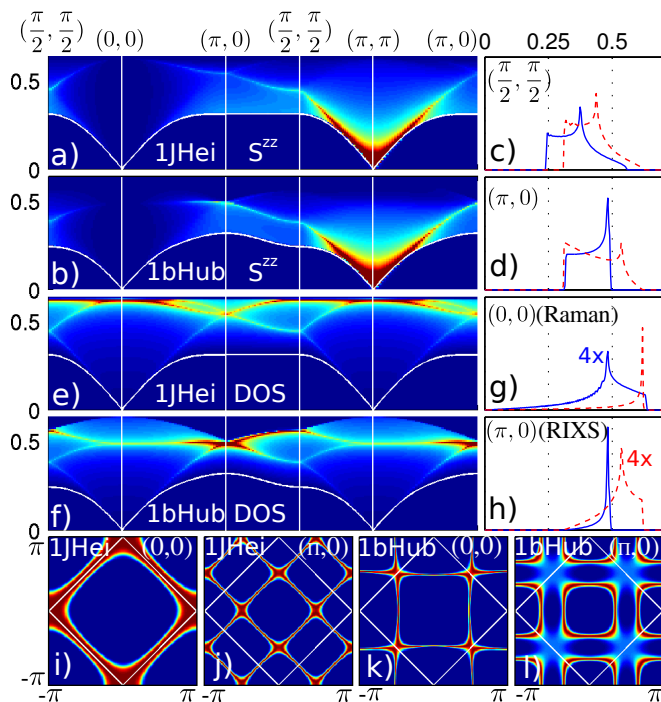


FIG. 4. (Color Online) (a-b) $S^{zz}(\mathbf{k}, \omega)$ for 1JHei with $J_{NN} = \omega_{(\pi,0)}/2Z_c$ and the 1bHub with the SCOC parameters. (c-d) S^{zz} energy lineshapes at the ZB points for 1JHei (dashed red line) and 1bHub (solid blue line). (e-f) Corresponding two-magnon DOS. (g-h) DOS profiles at $(0,0)$ and $(\pi,0)$. (i-j) Single magnons wave-vectors contributing to the DOS peaks at $(0,0)$ and $(\pi,0)$ in 1JHei, (k-l) in the SCOC 1bHub.

at $(\pi,0)$ [Fig. 4(d)] which shows that attempts to explain the reported INS lineshape at $(\pi,0)$ from quantum effects must consider the full Hamiltonian presented here [7, 18, 19]. Also, along the ZB, the intensity of the one-magnon (transverse) excitations is constant so that the missing spin-wave amplitude observed by INS [7, 18, 20, 21] *does not* result from further neighbor hopping.

In the 1JHei, the $(0,0)$ two-magnon DOS peaks at $4Z_c J_{NN}$, corresponding to creating two spin-waves at the ZB. The peak in Raman B_{1g} spectra is found at 0.37 eV for SCOC [22] corresponding to $\sim 2.8J_{NN}$. The reduced energy was explained as due to magnon-magnon interactions [16], but the peak-width could not be reproduced. The large ZB dispersion that our model entails firstly imply that experiments should not be compared to a single J_{NN} , secondly it explains the Raman peak width as a range of energies from $2\omega_{(\pi,0)}$ extending down to $2\omega_{(\frac{\pi}{2}, \frac{\pi}{2})}$, where a maximum occurs because at this energy entire lines in one-magnon momentum space contribute [Fig. 4(k)]. Thirdly, it predicts a lower peak energy requiring weaker magnon interaction to match experiments. For a correct calculation of magnon interactions, we caution that in the cuprates, it is different one-magnon that contribute to the Raman peak [Fig. 4(k)],

than in the 1JHei [Fig. 4(i)]. The observation of a strong excitation at $(\pi, 0)$ in K-edge RIXS [14] is also explained by our calculations, which demonstrate a concentration of DOS at exactly this wave-vector. Again the one-magnon states that contributes to this peak [Fig. 4(l)] are very different from the 1JHei [Fig. 4(j)]. Thus, our results reveal dramatic differences in the two-magnon continuum, implying that INS, L_3 or K-edge RIXS and Raman data must be interpreted using the full quantitative model derived here.

Our model also provide insight into the electronic spectra, such as the bare-band dispersion used to extract the self-energy function from ARPES spectra. A self-consistent Kramers-Kroniger analysis of ARPES experiments on Bi2212 revealed $t \simeq 0.23$ eV [23]. However, with the discovery of a high-energy kink [24] at 0.4 eV in the nodal spectrum (also known as the waterfall feature), a similar analysis on optimally doped LSCO [25] suggested that $t \simeq 0.48$ eV. Our results for LCO ($t = 0.492$ eV) support the second scenario.

In summary we derived an effective spin Hamiltonian valid for any lattice and any hopping matrix element range. Using spin-wave theory with $1/S$ -corrections and three hopping t , t' and t'' , we obtain accurate quantitative 1bHub parameter sets for several parent compounds of the high- T_c cuprate superconductors. We predict ordered moment, double occupancy, SW renormalization and 2-magnon spectra. From the non-interacting two-magnon $S^{zz}(\mathbf{q}, \omega)$ and DOS, we clearly demonstrate the necessity to include the extended exchange paths to interpret Raman and K-edge RIXS peaks. Furthermore, electronic spectra such as ARPES could also be addressed using the same 1bHub parameters.

We gratefully acknowledge Headings *et al.* [7] for sharing their data, J. Chang, F. Vernay, F. Mila, T. A. Tòth, B. Normand and M. E. Zhitomirsky for fruitful discussions, K. J. Zhou for his help with the RIXS experiment and the Swiss NSF and the MaNEP NCCR for support.

-
- [1] P. W. Anderson, *Science* **235**, 1196 (Mar. 1987).
 - [2] A. H. MacDonald *et al.*, *Phys. Rev. B* **37**, 9753 (Jun. 1988).
 - [3] R. Coldea *et al.*, *Phys. Rev. Lett.* **86**, 5377 (Jun. 2001).
 - [4] A. Damascelli *et al.*, *Rev. Mod. Phys.* **75**, 473 (Apr 2003).
 - [5] J. P. Delannoy *et al.*, *Phys. Rev. B* **79**, 235130 (Jun. 2009).
 - [6] Guarise *et al.*, *Phys. Rev. Lett.* **105**, 157006 (Oct 2010).
 - [7] Headings *et al.*, *Phys. Rev. Lett.* **105**, 247001 (Dec 2010).
 - [8] P. A. Lee *et al.*, *Rev. of Mod. Phys.* **78**, 17 (Jan 2006).
 - [9] T. Oguchi, *Phys. Rev.* **117**, 117 (Jan 1960).
 - [10] T. Tohyama and S. Maekawa, *Supercond. Sci. Technol.* **13**, R17 (Apr 2000).
 - [11] Y.-D. Chuang *et al.*, *Phys. Rev. B* **69**, 094515 (Mar 2004).

- [12] J. Lorenzana et al., Phys. Rev. B **72**, 224511 (Dec 2005).
- [13] M. Z. Hasan et al., Science **288**, 1811 (2000).
- [14] D. S. Ellis et al., Phys. Rev. B **81**, 085124 (Feb 2010).
- [15] C. M. Canali and M. Wallin, Phys. Rev. B **48**, 3264 (Aug 1993).
- [16] C. M. Canali and S. M. Girvin, Phys. Rev. B **45**, 7127 (Apr 1992).
- [17] T. Nagao and J.-I. Igarashi, Phys. Rev. B **75**, 214414 (Jun 2007).
- [18] N. B. Christensen et al., P. Natl. Acad. Sci. USA **104**, 15264 (2007).
- [19] N. Tsyrlin, F. Xiao, A. Schneidewind, P. Link, H. M. Ronnow, J. Gavilano, C. P. Landee, M. M. Turnbull, and M. Kenzelmann, Phys. Rev. B **81** (2010).
- [20] H. M. Rønnow, D. F. McMorrow, R. Coldea, A. Harrison, I. D. Youngson, T. G. Perring, G. Aeppli, O. Syljuåsen, K. Lefmann, and C. Rischel, Phys. Rev. Lett. **87**, 037202 (Jun 2001).
- [21] N. B. Christensen, D. F. McMorrow, H. M. Rønnow, A. Harrison, T. G. Perring, and R. Coldea, J. Mag. Mag. Mat. **272**, 896 (2004).
- [22] G. Blumberg et al., Phys. Rev. B **53**, R11930 (May 1996).
- [23] A. A. Kordyuk, S. V. Borisenko, A. Koitzsch, J. Fink, M. Knupfer, and H. Berger, Phys. Rev. B **71**, 214513 (Jun 2005).
- [24] J. Graf, G.-H. Gweon, K. McElroy, S. Y. Zhou, C. Jozwiak, E. Rotenberg, A. Bill, T. Sasagawa, H. Eisaki, S. Uchida, H. Takagi, D.-H. Lee, and A. Lanzara, Phys. Rev. Lett. **98**, 067004 (Feb 2007).
- [25] J. Chang et al., Phys. Rev. B **78**, 205103 (Nov 2008).

This figure "Fig1.png" is available in "png" format from:

<http://arxiv.org/ps/1104.4224v1>

This figure "Fig2.png" is available in "png" format from:

<http://arxiv.org/ps/1104.4224v1>

This figure "plaquette2.png" is available in "png" format from:

<http://arxiv.org/ps/1104.4224v1>

This figure "Fig3.png" is available in "png" format from:

<http://arxiv.org/ps/1104.4224v1>

This figure "plaquette3.png" is available in "png" format from:

<http://arxiv.org/ps/1104.4224v1>

This figure "Fig4.png" is available in "png" format from:

<http://arxiv.org/ps/1104.4224v1>

This figure "plaquette4.png" is available in "png" format from:

<http://arxiv.org/ps/1104.4224v1>